Bioorganic & Medicinal Chemistry 17 (2009) 1125–1131

Contents lists available at ScienceDirect

Bioorganic & Medicinal Chemistry

journal homepage: www.elsevier.com/locate/bmc

# Novel 6-methanesulfonamide-3,4-methylenedioxyphenyl-*N*-acylhydrazones: Orally effective anti-inflammatory drug candidates

Jorge L. M. Tributino [a,b], Carolina D. Duarte [a,c], Rodrigo S. Corrêa [d,e], Antonio C. Doriguetto [d], Javier Ellena [e], Nelilma C. Romeiro [a], Newton G. Castro [b], Ana Luisa P. Miranda [a], Eliezer J. Barreiro [a,b,c], Carlos A. M. Fraga [a,b,c,*]

[a] *LASSBio—Laboratório de Avaliação e Síntese de Substâncias Bioativas, Faculdade de Farmácia, Universidade Federal do Rio de Janeiro, PO Box 68023, 21941-902 Rio de Janeiro, RJ, Brazil*
[b] *Programa de Pós-Graduação em Farmacologia e Química Medicinal, Instituto de Ciências Biomédicas, Universidade Federal do Rio de Janeiro, Rio de Janeiro, RJ, Brazil*
[c] *Programa de Pós-Graduação em Química, Instituto de Química, Universidade Federal do Rio de Janeiro, Rio de Janeiro, RJ, Brazil*
[d] *Laboratório de Cristalografia, Departamento de Ciências Exatas, Universidade Federal de Alfenas—UNIFAL-MG, 37130-000 Alfenas, MG, Brazil*
[e] *Instituto de Física de São Carlos, Universidade de São Paulo, 13560-970 São Carlos, SP, Brazil*

ARTICLE INFO

*Article history:*
Received 13 September 2008
Revised 13 December 2008
Accepted 17 December 2008
Available online 25 December 2008

*Keywords:*
*N*-Acylhydrazone derivatives
Anti-inflammatory
Anti-hyperalgesic
COX-1 inhibitor
Safrole
1,3-Benzodioxole

ABSTRACT

We described herein the molecular design of novel in vivo anti-inflammatory 6-methanesulfonamide-3,4-methylenedioxyphenyl-*N*-acylhydrazone derivatives (**1**) planned by applying the molecular hybridization approach. This work also points out to the discovery of LASSBio-930 (**1c**) as a novel anti-inflammatory and anti-hyperalgesic prototype, which was able to reduce carrageenan-induced rat paw edema with an $ED_{50}$ of 97.8 μmol/kg, acting mainly as a non-selective COX inhibitor.



## 1. Introduction

Inflammation can be defined as an intricate response from damaged tissue, which consists in assembled interactions among cell-derived mediators leading to recovery. Conversely, in pathological conditions evolving persistent tissue damage by inflammatory cells, repair is not suitably accomplished.[1] Eicosanoids, important mediators of the inflammatory process, are able to activate and sensibilize nociceptors, leading to hyperalgesia[2] and their role in the genesis of several pathological states, such as chronic inflammatory diseases, thrombosis and pain, is well established.[3]

In the recent literature, we have described the structure–activity relationships of numerous series of *N*-acylhydrazones (NAH), with potent anti-inflammatory, antinociceptive and antiplatelet activities.[4,5] The relative acidity of the amide hydrogen of the NAH function, as well as its capacity for stabilizing free radicals give these compounds the ability of mimicking the bis-allylic moiety of unsaturated fatty acids and amides, for example, arachidonic acid (AA).[6] In addition, we have previously reported the synthesis and anti-inflammatory properties of orally active flosulide analogues derived from natural safrole.[7] More recently, Khanapure et al.[8] described methaaryl and methacycloalkyl derivatives and ketone analogues, structurally related to our flosulide analogues, as potent cycloxygenase-2 (COX-2) inhibitors, anti-inflammatory agents.

Our present work describes the development of novel drug candidates with an orally active anti-inflammatory and analgesic profile, based on our previous results concerning the medicinal chemistry of NAH and 1,3-benzodioxole-containing derivatives.[4–7] Aiming to optimize the NAH privileged scaffold[9] to achieve more effective anti-inflammatory compounds, the rational approach leading to the new 6-methanesulfonamide-3,4-methylenedioxyphenyl-*N*-acylhydrazones (**1a–d**) included molecular hybridization of LASSBio-294 (**2**), a potent analgesic and antiplatelet derivative but poor anti-inflammatory,[10] and LASSBio-259 (**3**), a flosulide analogue with potent in vivo anti-inflammatory properties.[7] The design concept of compounds (**1a–d**) explored the introduction of a methanesulfonamide group in the 1,3-benzodioxole ring at position 6 and the NAH moiety working as a linker between the two peripheral aromatic rings (Scheme 1). The nature of the aryl groups attached to the imine subunit of the new series of compounds (**1a–d**), that is 2-furyl, 2-thiophenyl and phenyl, was elected based on classical ring

* Corresponding author. Tel.: +55 21 25626503; fax: +55 21 25626644.
*E-mail address:* cmfraga@pharma.ufrj.br (C.A.M. Fraga).

0968-0896/$ - see front matter © 2009 Elsevier Ltd. All rights reserved.
doi:10.1016/j.bmc.2008.12.045

isosteric replacement[11] while 3,5-di-*tert*-butyl-4-hydroxyphenyl was elected aiming at introducing the characteristic redox properties of this moiety into the new series of compounds, as previously reported for other series of bioactive NAH derivatives.[5f]

## 2. Results and discussion

### 2.1. Chemistry

For the synthesis of the new substituted 6-methanesulfonamide-3,4-methylenedioxyphenyl-*N*-acylhydrazone derivatives (**1**), an abundant natural product from Brazilian flora, that is, safrole (**4**, Scheme 2)[12] was used as starting material. As recently described by our group,[5f] 6-nitropiperonyl methyl ester (**5**) was prepared in 63% yield from safrole (4 steps), by means of isomerization and oxidative cleavage,[13] nitration[14] and Yamada's oxidation conditions.[15] The regioselective introduction of the nitro group was clearly evidenced by usual spectroscopic methods as previously described.[5f,14]

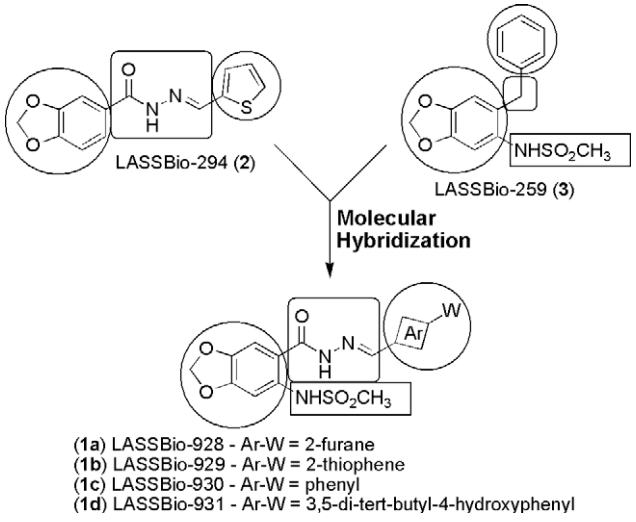


**Scheme 1.** Design concept for 6-methanesulfonamide-3,4-methylenedioxyphenyl-*N*-acylhydrazone derivatives (**1a–d**).

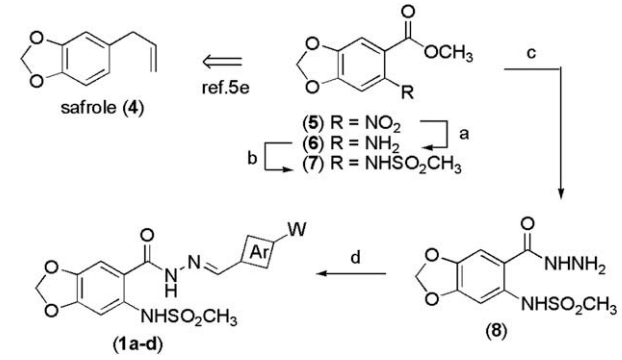


**Scheme 2.** Synthesis of 1,3-benzodioxole NAH derivatives (**1a–d**). Reagents and conditions: (a) $Fe^0$, $NH_4Cl$, EtOH/$H_2O$, reflux, 2 h, 75%; (b) $CH_3SO_2Cl$, Py, $CH_2Cl_2$, rt, 1 h, 89%; (c) $N_2H_4{\cdot}H_2O$ 80%, EtOH, rt, 1 h, 78%; (d) ArCHO, EtOH, rt, 0.5 h, 70–88%.

The nitro-ester (**5**) was then submitted to chemoselective nitro group reduction with metallic iron in acidic media,[7] affording the corresponding aniline derivative (**6**) in 75% yield. Further mesylation reaction[7] furnished the corresponding *N*-methanesulfonyl derivative (**7**) in 89% yield. Infrared spectra of the former compound shows absorption bands in 3140 and 3108 $cm^{-1}$ referring to axial deformation of N–H, whilst 1675, 1362 and 1148 $cm^{-1}$ bands are characteristic of carbonyl group deformation and asymmetric and symmetric deformations of the $-SO_2$ group, respectively.

The key hydrazide intermediate (**8**) was then obtained in 78% yield, by treating an ethanolic solution of (**7**) with hydrazine hydrate at room temperature for 1 h.[5e] Finally, subsequent condensation with the appropriate aromatic aldehydes in ethanol[5e] provided the new NAH target compounds (**1a–d**) (Table 1), under acid catalysis, in 22–27% overall yield from (**4**). The careful analysis of $^1H$ NMR spectra (Table 1) of the obtained NAH (**1**) indicated that the condensation reaction was highly diastereoselective since only the *E*-diastereomer at the imine double bond level was evidenced, in agreement with our previous results.[5]

In order to assure unambiguously the relative configuration of the diastereomer obtained during the synthesis of these new 1,3,benzodioxole NAH derivatives, essential to the understanding of the biological results, we have selected the unsubstituted compound LASSBio-930 (**1c**), to investigate the geometric isomerism and other conformational factors by X-ray diffraction.

The ORTEP-3[16] view of LASSBio-930 (**1c**) with the atom numbering scheme is shown in Figure 1. The main geometric parameters are given in Supplementary data. There are two molecular moieties, which are individually almost flat: the moiety 1 containing the atoms C8 and N3 and those ones present in rings A and B; and the moiety 2 containing ring C and N1, N2 and C9. The largest deviations from the least squares plane through the moieties 1 and 2 are 0.036(2) and −0.046(2) Å for N1 and C8 atoms, respectively. The least squares planes of the moieties 1 and 2 form an angle of 13.4(1)°. This geometric feature is also highlighted by the torsional angle considering C6–C1–C8–N2 (torsion = 22.0(1)°). The O1 atom is slightly closer to the planar moiety 2 (0.323(2) Å) than the planar moiety 1 (0.371(3) Å). Another important intra-molecular information revealed by the X-ray crystallographic analysis is the orientation of the methanesulfonamide group. The S1 and O6 atoms deviate 0.229(2) and 0.122(3) Å from the least squares plane through the moiety 1, whereas for the O5 and C22 atoms the deviations are −0.671(3) and 1.853(3) Å, respectively.

**Table 1**
Yields and physicochemical properties of new 6-methanesulfonamide-3,4-methylenedioxyphenyl-*N*-acylhydrazone NAH derivatives (**1a–d**)

| Compound | Yield[a] (%) | Molecular formula[b] | Melting point[c] (°C) | $\Delta$[d] (ppm) | | |
|---|---|---|---|---|---|---|
| | | | | CON*H* | $SO_2N$*H* | N=*CH* |
| **1a** | 86 | $C_{14}H_{13}N_3O_6S$ | 260–262 | 11.8 | 10.6 | 7.1 |
| **1b** | 88 | $C_{14}H_{13}N_3O_5S_2$ | 276–278 | 11.8 | 10.6 | 7.3 |
| **1c** | 84 | $C_{16}H_{15}N_3O_5S$ | 244–246 | 11.9 | 10.7 | 8.4 |
| **1d** | 70 | $C_{24}H_{31}N_3O_6S$ | 254–255 | 11.7 | 10.7 | 8.3 |

[a] Isolated yield.
[b] The analytical results for C,H,N were within ±0.4% of calculated values.
[c] Not corrected.
[d] Data obtained $^1H$ NMR at 200 MHz, using DMSO-$d_6$ as solvent.

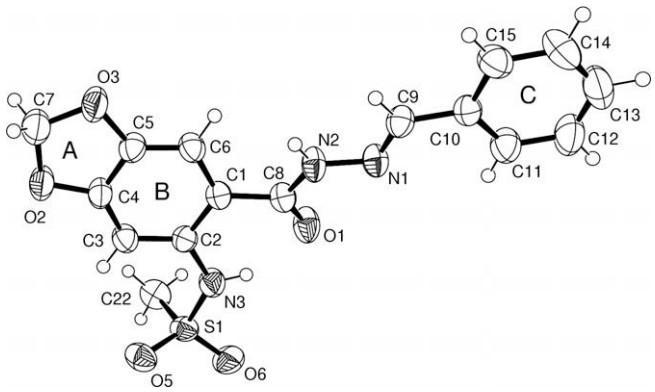


**Figure 1.** ORTEP view of LASSBio-930 (**1c**) showing the arbitrary atom labelling. Ellipsoids represent 50% probability level.

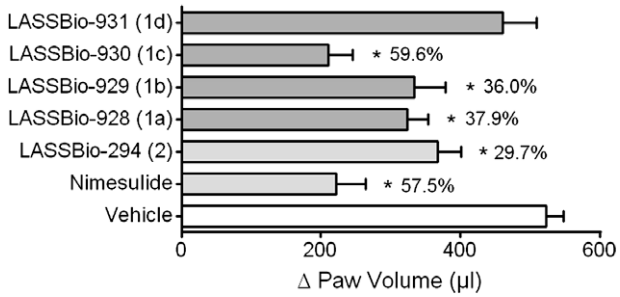


**Figure 2.** Anti-inflammatory evaluation of 6-methanesulfonamide-3,4-methylenedioxyphenyl-*N*-acylhydrazone (**1a**–**d**) on carragenaan-induced rat paw edema. Results refer to the 3rd hour paw volumes after carrageenan-challenge and are expressed in terms of mean ± SEM ($n$ = 8–10 animals per group). Compounds were administered orally at a dose of 300 µmol/kg. $^{*}p < 0.05$ compared to the vehicle group (Student $t$ test).

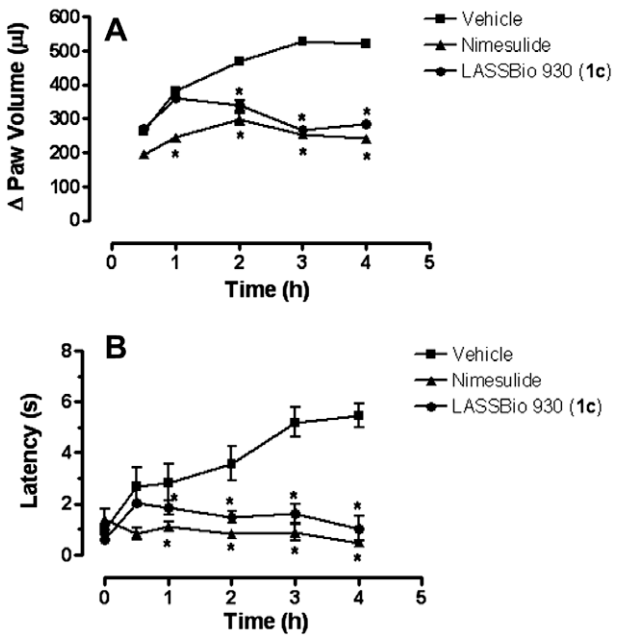


**Figure 3.** Time course effect of LASSBio-930 (**1c**) and nimesulide on carrageenan-induced rat paw edema (A) and thermal hyperalgesia (B). Results are expressed in terms of mean ± SEM ($n$ = 8–10 animals per group). LASSBio-930 and nimesulide (300 µmol/kg; p.o.). $^{*}p < 0.05$ compared to the vehicle control group (Student's $t$ test).

The compound LASSBio-930 (**1c**) exhibits a moderate intramolecular hydrogen bond involving N3–H1···O1. The weak intermolecular hydrogen bond between O5 in the methanesulfonamide and the adjacent hydrogen donor group N2–H2 at $-x$, $-y+1$, $-z$ helps in the packing stabilization and gives rise to the dimer. The remaining O atom present in the methanesulfonamide subunit, O6, also contributes to the packing stabilization forming bifurcated non-classical H bonds (C9–H9···O6 and C22–H22C···O6). Another non-classical inter-molecular hydrogen bond occurs between C7–H7A···O2, which forms a centrosymmetrical dimer linked by the heterocyclic five membered ring. All information concerning the inter-molecular geometry are given in the Supplementary data.

## 2.2. Pharmacology

For the in vivo pharmacological evaluation of the new substituted 6-methanesulfonamide-3,4-methylenedioxyphenyl-*N*-acylhydrazone derivatives (**1a–d**), we elected the carrageenan-induced rat paw edema model (CIRPE), a classic model of acute inflammation[17] (Fig. 2). Nimesulide, a diarylether anti-inflammatory drug and LASSBio-294 (**2**) were used as standards. All compounds were administered orally (300 µmol/kg) 1 h before inflammatory challenge.

The new compounds LASSBio-928 (**1a**), LASSBio-929 (**1b**) and LASSBio-930 (**1c**) were more effective on rat paw edema prevention than prototype LASSBio-294 (**2**). These results point out to the importance of the methanesulfonamide group at C6 of the 1,3-benzodioxole ring for the improvement of anti-inflammatory activity. However, LASSBio-931 (**1d**), the 3,5-di-*tert*-butyl-4-hydroxyphenyl derivative, did not show a significant anti-inflammatory effect (Fig. 2), which may have been the result of a higher lipophilicity and lower solubility of this compound as compared to the other ones, which could contribute to differences in their bioavailability.

Moreover, the most active compound on this pharmacological protocol (ca. 60% inhibition), that is, LASSBio-930 (**1c**), presented a dose-dependent profile with an $ED_{50}$ = 97.8 µmol/kg and effectiveness similar to the standard drug nimesulide.[18] The edema was inhibited from the 2nd hour after carrageenan injection. LASSBio-930 also demonstrated an anti-inflammatory effect on the arachidonic acid-induced ear edema (data not shown). For this reason, compound (**1c**) can be considered as the representative hybrid analog of LASSBio-259 (**3**) where the methylene spacer was substituted by the NAH moiety from LASSBio-294 (**2**) (Scheme 1).

Additionally, LASSBio-930 (**1c**) was able to reduce significantly the associated hyperalgesia induced by carrageenan in the same model (Fig. 3), corroborating the preliminary antinociceptive activity demonstrated by means of the inhibition of the AcOH-induced constrictions by 70% at 300 µmol/kg and with the inhibition of the inflammatory phase of the formalin-induced hyperalgesia test, both in mice (Fig. 4). Carragenan-induced inflammation is characterized by the production of $PGE_2$ in tissues resulting in hyperalgesia. Thus, it has been demonstrated that NSAIDs like indomethacin and nimesulide are able to inhibit paw edema production and thermal hyperalgesia.[19,20]

In order to investigate if the anti-inflammatory profile of LASSBio-930 (**1c**) was dependent on COX blockage, we evaluated its ability to inhibit the isoforms 1 and 2 of this enzyme by using the human whole blood (HWB) in vitro assay.[21,22] COX-1 activity was measured through $TXB_2$ production in a spontaneous human whole blood clot assay and COX-2 activity through $TXB_2$ production from whole blood samples stimulated by lipopolysaccharide (LPS). The $IC_{50}$ values for COX's and the selectivity index were determined for LASSBio-930 (**1c**) and nimesulide, as summarized in Table 2.

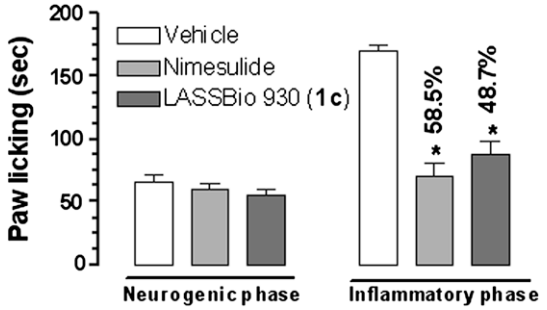


**Figure 4.** Effect of LASSBio-930 (**1c**) and nimesulide in mice formalin-induced pain test. Each column represents the mean ± SEM ($n$ = 8 animals per group). LASSBio-930 and nimesulide (300 μmol/kg; p.o). $^{*}p < 0.05$ compared to the vehicle control group (Student's $t$ test).

**Table 2**
In vitro COX-1 and COX-2 human whole blood inhibition assay for LASSBio-930 (**1c**) and nimesulide

| Compound | HWB $IC_{50}$[a] (μM) | | Selectivity index $^{IC}_{50}$COX-1/$^{IC}_{50}$COX-2 |
|---|---|---|---|
| | COX-1 | COX-2 | |
| Nimesulide | 10.9 ± 1.2 | 3.5 ± 1.3 | 3.1 |
| LASSBio-930 (**1c**) | 4.1 ± 1.1 | 10.2 ± 1.3 | 0.4 |

[a] $IC_{50}$ values (i.e., the concentration able to elicit 50% of the maximum effect observed) were determined by non-linear regression using GraphPad Prism software. Each point of the curve represents the mean ± SEM of the % of inhibition of $TXB_2$ formation ($n$ = 3–5 independent experiments). Concentration range for COX-1 (0.01–500 μM). Concentration range for COX-2 (0.001–1000 μM).

The obtained results showed that LASSBio-930 (**1c**) presented a COX-1 and COX-2 inhibitory profile similar to that observed for nimesulide, as previously anticipated from our in vivo CIRPE results, with an inverse selectivity profile (SI = 0.4 and 3.1, respectively) (Table 2). Additionally, in spite of the presence of the methanesulfonamide subunit in the hybrid analogue LASSBio-930 (**1c**), classically known as a pharmacophoric group for COX-2 inhibition,[23] it has proven to be a better COX-1 inhibitor ($IC_{50}$ = 4.1 μM).

## 2.3. Molecular docking

Aiming to support the in vitro COX inhibitory profile displayed by LASSBio-930 (**1c**) and nimesulide we performed molecular docking studies using available COX-1 and COX-2 X-ray crystal structures with bound inhibitors.[24,25] This theoretical study was performed using the genetic algorithm-based docking program GOLD.[26] The proposed binding modes of the ligand into the active site of COX-1 and COX-2 were determined as the best ranked compounds according to ChemScore scoring function,[27] which corresponds to the structure with the most favourable free energy of binding, that is, $\Delta G_{binding}$ (kJ/mol) (Table 3).

The $\Delta G_{binding}$ values obtained reveal that nimesulide has a slight preference for binding COX-2, with a small difference of 1.52 kJ/mol, as it is observed experimentally. The same feature was observed for LASSBio-930, except that its binding to COX-1 is energetically more favourable than to COX-2 by 2.82 kJ/mol (Table 3). These results suggest a non-selective profile for this compound, as has been observed in the in vitro pharmacological assays, since the energy difference is so small.

The visual analysis of the docked complexes between LASSBio-930 and COX-1 (Fig. 5A) shows that LASSBio-930 is able to form one hydrogen bond involving the hydrogen atom of the imine moiety and the hydroxyl of Ser530.

**Table 3**
$\Delta G_{binding}$ values (kJ/mol) obtained for LASSBio-930 (**1c**) and nimesulide through Chemscore function in GOLD program

| Compound | $\Delta G_{binding}$ | |
|---|---|---|
| | COX-1 | COX-2 |
| Nimesulide | −31.75 | −33.27 |
| LASSBio-930 (**1c**) | −39.85 | −37.03 |

However, the visual inspection of the best-ranked complex of LASSBio-930 with COX-2 (Fig. 5B) shows an inverted putative binding mode in comparison to COX-1, in which there is one hydrogen bond between one of the oxygen atoms of the sulfonamide group and the guanidine group of Arg120. Although these observations suggest more favourable polar interactions of LASSBio-930 with COX-2 than COX-1, which is not evidenced by the $\Delta G_{binding}$ energy term, $\Delta G_{lipo}$ values obtained for COX-1 and this compound (data not labeled) are more favourable than for COX-2 (249.10 vs 233.83 kJ/mol, respectively), suggesting more favourable hydrophobic interactions between LASSBio-930 and COX-1 and corroborating the low COX-1-selective profile observed experimentally for this compound.

## 3. Conclusions

LASSBio-930. (**1c**) was identified as a new anti-inflammatory and anti-hyperalgesic prototype belonging to the methanesulfonamide *N*-acylhydrazone series, which exert their bioactivities through non-selective COX inhibition. This compound was elected for further pharmacological evaluation on chronic inflammation and pain models in order to confirm its potential as a drug candi-

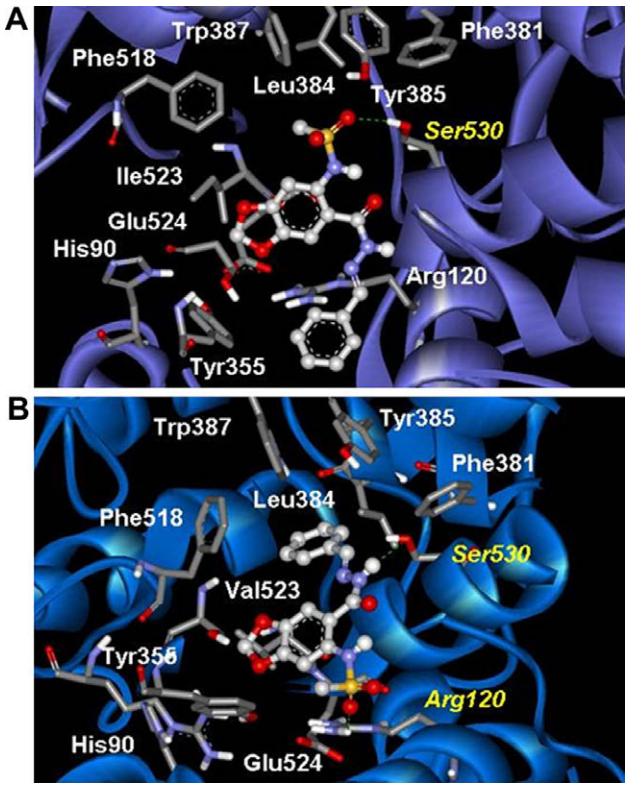


**Figure 5.** Best-ranked LASSBio-930-COX-1 (A) and LASSBio-930-COX-2 (B) binding poses as obtained by docking with ChemScore scoring function. Hydrogen bonds are shown as green dashed lines. Hydrogen-bonding interacting residues are labeled yellow. Only polar hydrogens are shown for clarity.

date for treatment of different inflammatory diseases and these results will be disclosed in a forthcoming paper.

## 4. Experimental

### 4.1. Chemistry

Reactions were routinely monitored by thin-layer chromatography (TLC) in Silica Gel (F245 Merck plates) and the products visualized with iodine or ultraviolet lamp (254 and 365 nm). $^1$H and $^{13}$C nuclear magnetic resonance (NMR) spectra were determined in DMSO-$d_6$ solutions using a Bruker AC-200 spectrometer. Peak positions are given in parts per million ($\delta$) from tetramethylsilane as internal standard, and coupling constant values ($J$) are given in Hertz. Infrared (IR) spectra were obtained using a Nicolet Magna IR 760 spectrometer. Samples were examined as potassium bromide (KBr) disks. Melting points were determined using a Quimis instrument and are uncorrected. Column chromatography purifications were performed using silica gel Merck 230–400 mesh. All organic solutions were dried over anhydrous sodium sulfate and all organic solvents were removed under reduced pressure in rotatory evaporator.

#### 4.1.1. Methyl 6-amino-1,3-benzodioxole-5-carboxylate (6)[7]

A mixture of 1.0 g (4.40 mmol) of methyl 6-nitro-1,3-benzodioxole-5-carboxylate (**5**), 1.39 g (24.9 mmol) of powder metallic iron and 0.14 g (2.70 mmol) of ammonium chloride suspended in 75 mL of ethanol/water (2:1) was refluxed for 1 h, when TLC indicated the end of the reaction. Then, the reaction mixture was filtered over Celite® and the filtrate was concentrated under reduced pressure, furnishing a crude dark yellow solid. Recrystallization from ethanol/water, afforded the title compound as a yellow solid (0.65 g, 75%), mp 175–176 °C. $^1$H NMR (200 MHz, $CDCl_3$, TMS) $\delta$ (ppm): 3.83 (s, 3H, OC$H_3$); 5.60 (s, 2H, N$H_2$); 5.89 (s, 2H, H-2); 6.17 (s, 1H, H-4); 7.26 (s, 1H, H-7). $^{13}$C NMR (50 MHz, $CDCl_3$, TMS) $\delta$ (ppm): 51.3 (O$CH_3$); 96.8 (C-2); 101.2 (C-7); 102.5 (C-4); 108.5 (C-5); 139.1 (C-6); 148.8 (C-3a); 152.9 (C-1a); 168.2 (C=O).

#### 4.1.2. Methyl 6-[(methylsulfonyl)amino]-1,3-benzodioxole-5-carboxylate (7)[7]

To a solution of 0.5 g (2.60 mmol) of (**6**) in 30 mL of dichoromethane containing 3.0 mL of anhydrous pyridine, was added 0.9 mL (11.60 mmol) of freshly distilled mesyl chloride. The reaction mixture was kept in room temperature for 1 h, when TLC indicated the end of the reaction. Then, the organic media was sequentially washed with 10% aq HCl (3 × 30 mL), saturated $CuSO_4$ solution (2 × 30 mL) and water (2 × 30 mL), dried and concentrated under reduced pressure to furnish (**7**) as a white solid (0.62 g, 89%), mp 178–180 °C. $^1$H NMR (200 MHz, $CDCl_3$, TMS) $\delta$ (ppm): 3.02 (s, 3H, $SO_2CH_3$); 3.91 (s, 3H, OC$H_3$); 6.05 (s, 2H, H-2); 7.31 (s, 1H, H-4); 7.44 (s, 1H, H-7); 10.00 (s, 1H, N$H$). $^{13}$C NMR (50 MHz, $CDCl_3$, TMS) $\delta$ (ppm): 40.0 ($SO_2CH_3$); 52.6 (O$CH_3$); 100.6 (C-2); 102.5 (C-7); 108.9 (C-4); 109.6 (C-5); 138.2 (C-6); 143.8 (C-3a); 153.2 (C-1a); 168.2 (C=O). IR (KBr) $\nu$ (cm$^{-1}$): 3140, 3108, 3017, 2952, 2932, 2852, 1675, 1627, 1507, 1486, 1443, 1362, 1332, 1244, 1148, 1030, 978, 903, 880, 784, 647, 500.

#### 4.1.3. *N*-[6-(hydrazinylcarbonyl)-1,3-benzodioxol-5-yl]methanesulfonamide (8)[5e]

To a solution of 0.5 g (1.80 mmol) of (**7**) in 10 mL of ethanol, was added 5.8 mL (92.8 mmol) of 80% hydrazine monohydrate. The reaction mixture was kept in room temperature for 1 h, when TLC indicated the end of the reaction. Then, the media was neutralized with concentrated HCl in an ice bath and the resulting precipitate was filtered out and recrystallized from ethanol/water, affording the desired compound (**8**) as a yellow solid (0.39 g, 78%), mp 198–200 °C. $^1$H NMR (200 MHz, DMSO-$d_6$, TMS) $\delta$ (ppm): 3.03 (s, 3H, $SO_2CH_3$); 4.60 (s, 2H, N$H_2$); 6.10 (s, 2H, H-2); 7.06 (s, 1H, H-4); 7.32 (s, 1H, H-7); 9.96 (s, 1H, $SO_2NH$); 11.29 (s, 1H, CONHNH$_2$). $^{13}$C NMR (50 MHz, DMSO-$d_6$, TMS) $\delta$ (ppm): 40.0 ($SO_2CH_3$); 101.8 (C-2); 102.7 (C-7); 107.2 (C-4); 113.0 (C-5); 135.4 (C-6); 143.9 (C-3a); 150.8 (C-1a); 167.4 (C=O).

#### 4.1.4. General procedure for preparation of 6-methanesulfonamide-*N*′-arylidene-1,3-benzodioxole-5-carbohydrazines (1a–d)[5e]

To a solution of 1 mmol of the hydrazide (**8**) in absolute ethanol (10 mL) containing two drops of 37% hydrochloric acid, was added 1.1 mmol of corresponding aromatic aldehyde derivative. The mixture was stirred at room temperature for 1 h, after then extensive precipitation was visualized. Next, the mixture was poured into cold water, neutralized with 10% aqueous sodium bicarbonate solution and the precipitate formed was filtered out and recrystallized from ethanol/water.

#### 4.1.5. *N*-(6-{[(2*E*)-2-(Furan-2-ylmethylidene)hydrazinyl]carbonyl}-1,3-benzodioxol-5-yl)methanesulfonamide (LASSBio-928, 1a)

The derivative (**1a**) was obtained in 86% yield, as a light yellow solid, mp 260–262 °C. $^1$H NMR (200 MHz, DMSO-$d_6$, TMS) $\delta$ (ppm): 3.08 (s, 3H, $SO_2CH_3$); 6.15 (s, 2H, H-2); 6.65 (s, 1H, H-4″); 6.95 (s, 1H, H-3″); 7.05 (s, 1H, H-4′); 7.41 (s, 1H, H-4); 7.85 (s, 1H, H-5″); 8.28 (s, 1H, H-7); 10.60 (s, 1H, $SO_2NH$); 11.77 (s, 1H, H-2′). $^{13}$C NMR (50 MHz, DMSO-$d_6$, TMS) $\delta$ (ppm): 40.3 ($SO_2CH_3$); 102.9 (C-2); 108.7 (C-3″); 112.7 (C-4″); 114.5 (C-7); 114.9 (C-5″); 135.2 (C-5); 138.8 (C-4′); 144.1 (C-6); 145.9 (C-4); 149.7 (C-1a); 151.0 (C-3a); 164.4 (C-1′).

#### 4.1.6. *N*-(6-{[(2*E*)-2-(Thiophen-2-ylmethylidene)hydrazinyl]carbonyl}-1,3-benzodioxol-5-yl)methanesulfonamide (LASSBio-929, 1b)

The derivative (**1b**) was obtained in 82% as a light yellow solid, mp 276–278 °C. $^1$H NMR (200 MHz, DMSO-$d_6$, TMS) $\delta$ (ppm): 3.08 (s, 3H, $SO_2CH_3$); 6.14 (s, 2H, H-2); 7.12 (d, 1H, $J$ = 4 Hz, H-4″); 7.16 (d, 1H, $J$ = 4 Hz, H-3″); 7.33 (s, 1H, H-4′); 7.42 (s, 1H, H-4); 7.69 (d, 1H, $J$ = 4 Hz, H-5″); 8.59 (s, 1H, H-7); 10.59 (s, 1H, $SO_2NH$); 11.81 (s, 1H, H-2′). $^{13}$C NMR (50 MHz, DMSO-$d_6$, TMS) $\delta$ (ppm): 40.2 ($SO_2CH_3$); 102.8 (C-2); 102.9 (C-3″); 108.1 (C-4″); 114.9 (C-5); 128.4 (C-7); 129.8 (C-5″); 131.9 (C-4′); 135.2 (C-6); 139.3 (C-1a); 144.1 (C-4); 151.0 (C-3a); 164.3 (C-1′).

#### 4.1.7. *N*-(6-{[(2E)-2-Benzylidenehydrazinyl]carbonyl}-1,3-benzodioxol-5-yl)methanesulfonamide (LASSBio-930, 1c)

The derivative (**1c**) was obtained in 95%, as a yellow solid, mp 244–246. $^1$H NMR (200 MHz, DMSO-$d_6$, TMS) $\delta$ (ppm): 3.09 (s, 3H, –$SO_2CH_3$); 6.15 (s, 2H, H-2); 7.12 (s, 1H, H-4); 7.46 (m, 4H, H-2″,3″,5″,6″); 7.73 (m, 2H, H-7,4″); 8.41 (s, 1H, H-4′); 10.66 (s, 1H, –$SO_2NH$); 11.87 (s, 1H, H-2′). $^{13}$C NMR (50 MHz, DMSO-$d_6$, TMS) $\delta$ (ppm): 40.3 (–$SO_2CH_3$); 102.8 (C-7); 102.9 (C-2); 108.1 (C-4); 114.8 (C-5); 127.7 (C-2″,6″); 129.4 (C-3″,5″); 130.8 (C-4″); 134.6 (C-1″); 135.4 (C-6); 144.0 (C-3a); 149.1 (C-4′); 151.1 (C-1a); 164.5 (C-1′).

#### 4.1.8. *N*-(6-{[(2*E*)-2-(4-Hydroxy-3,5-di-*tert*-butyl-benzylidene)hydrazinyl]carbonyl}-1,3-benzodioxol-5-yl)methanesulfonamide (LASSBio-931, 1d)

The derivative (**1d**) was obtained in 70% yield, as a yellow solid, mp 254–255. $^1$H NMR (200 MHz, DMSO-$d_6$, TMS) $\delta$ (ppm): 1.41 (s, 18H, –C($CH_3$)$_3$); 3.08 (s, 3H, –$SO_2CH_3$); 6.14 (s, 2H, H-2); 7.11 (s, 1H, –O$H$); 7.46 (m, 4H, H-4,7,2″,6″); 8.32 (s, 1H, H-4′); 10.73 (s, 1H, –$SO_2NH$); 11.67 (s, 1H, H-2′). $^{13}$C NMR (50 MHz, DMSO-$d_6$, TMS) $\delta$ (ppm): 33.7 (–C($CH_3$)$_3$); 38.1 (–$SO_2CH_3$); 43.3 (–$C$($CH_3$)$_3$); 105.8 (C-7); 106.0 (C-2); 111.2 (C-4); 117.9 (C-5); 127.7 (C-2″,6″); 128.9 (C-3″,5″); 138.4 (C-1″); 142.8 (C-6); 147.1 (C-1a); 153.7 (C-4′); 154.0 (C-3a); 160.0 (C-4″); 167.3 (C-1′).

### 4.2. Single crystal X-ray diffraction

After the synthesis and purification procedures, a well-shaped clear single crystal of (LASSBio-930), which was grown by recrystallization from 1:1 dichloromethane and methanol mixture, was selected for the X-ray diffraction experiment. Intensity data were measured with the crystal at room temperature (298 K) and with graphite monochromated Mo Kα radiation ($\lambda$ = 0.71073 Å), using the Enraf-Nonius Kappa-CCD diffractometer. The cell refinements were performed using the software COLLECT[28] and SCALEPACK,[29] and the final cell parameters were obtained on all reflections. Data reduction was carried out using the software DENZO-SMN and SCALEPACK. Since the absorption coefficient is insignificant (0.232 $mm^{-1}$), no absorption correction was applied.

The structure was solved using the software SHELXS-97[30] and refined using the software SHELXL-97.[31] Non-hydrogen atoms of the molecules were clearly solved and full-matrix least-squares refinement of these atoms with anisotropic thermal parameters was carried on. The C–H hydrogen atoms were positioned stereochemically and were refined with fixed individual displacement parameters [$U_{iso}$(H) = 1.2$U_{eq}$ ($C_{sp^2}$) or 1.5$U_{eq}$ ($C_{sp^3}$)] using a riding model with aromatic C–H bond length of 0.93 Å, methyl C–H one of 0.96 Å and methylene C–H one of 0.97 Å. The H atoms linked to nitrogen of the methanesulfonamide group were located by difference Fourier synthesis and were set as isotropic. Crystal, collection and structure refinement data are summarized in Table 4. Tables were generated by WINGX[32] and the structure representations by ORTEP-3[16] and MERCURY.[33]

Atomic coordinates, bond lengths, angles and thermal parameters have been deposited at the Cambridge Crystallographic Data Center, deposition number CCDC 658937.

**Table 4**
Crystal data and structure refinement for NAH derivative LASSBio-930 (**1c**)

| | |
|---|---|
| Empirical formula | $C_{16}H_{15}N_3O_5S_1$ |
| Formula weight | 361.37 |
| Temperature (K) | 298(2) |
| Wavelength (Å) | 0.71073 |
| Crystal system | Monoclinic |
| Space group | $P2_1/c$ |
| *Unit cell dimensions* | |
| $a$ (Å) | 11.2724(4) |
| $b$ (Å) | 8.4786(2) |
| $c$ (Å) | 17.1899(5) |
| $\alpha$ (°) | 90 |
| $\beta$ (°) | 97.463(1) |
| $\gamma$ (°) | 90 |
| Volume (Å$^3$) | 1628.99(8) |
| $Z$ | 4 |
| $D_{calcd}$ (Mg/m$^3$) | 1.473 |
| Absorption coefficient ($mm^{-1}$) | 0.232 |
| $F$(000) | 752 |
| Crystal size (mm$^3$) | 0.16 × 0.08 × 0.03 |
| $\theta$ Range for data collection (°) | 3.19–27.48 |
| Index ranges | $-12 \leqslant h \leqslant 14$, $-10 \leqslant k \leqslant 10$, $-22 \leqslant l \leqslant 21$ |
| Reflections collected | 24,557 |
| Independent reflections | 3709 [$R$(int) = 0.0620] |
| Completeness to $\theta$ = 27.48° | 99.3% |
| Max. and min. transmission | 0.9931 and 0.9638 |
| Refinement method | Full-matrix least-squares on $F^2$ |
| Data/restraints/parameters | 3709/0/231 |
| Goodness-of-fit on $F^2$ | 1.016 |
| Final $R$ indices [$I > 2\sigma(I)$] | $R_1$ = 0.0474, $wR_2$ = 0.1072 |
| $R$ indices (all data) | $R_1$ = 0.0973, $wR_2$ = 0.1308 |
| Largest diff. peak and hole (e Å$^{-3}$) | 0.203 and −0.396 |

### 4.3. Pharmacology

#### 4.3.1. Carragenaan-induced rat paw edema and hyperalgesia assay[34,35]

Fasted Wistar rats of both sexes (150–200 g) were used. Compounds were administered orally (300 μmol/kg; 0.1 mL/20 g) as a suspension in 5% arabic gum in saline (vehicle). Control animals received an equal volume of vehicle. One hour later, the animals were injected with either 0.1 mL of 1% carrageenan solution in saline (1 mg/paw) or sterile saline (NaCl 0.9%), into the subplantar surface of one of the hind paws respectively. The paws volumes were measured temporally and at the 3rd hour after the subplantar injection using a glass plethysmometer coupled to a peristaltic pump. The edema was calculated as the volume variation between the carrageenan and saline treated paw. Nimesulide (300 μmol/kg) was used as standard drug in the same conditions. Anti-inflammatory activity was expressed as % of inhibition of the edema when compared with the vehicle control group. The thermal hyperalgesia is determined using the modified hot-plate test[35] in the same animals used for edema assay. Rats are placed individually on a hot plate with the temperature adjusted to 51 °C. The latency of the withdrawal response of the left hind paw is determined at 0, 30, 60, 120, 180 and 240 min post-challenge. The time of maximum permanence permitted on the hot surface is 20 s. Hyperalgesia to heat is defined as a decrease in withdrawal latency and calculated as follows: $\Delta$ paw withdrawal latency (s) = (left paw withdrawal latency at time 0) − (left paw withdrawal latency at the others times).

### 4.4. Human whole blood assay

#### 4.4.1. In vitro COX-1 assay[21]

Briefly, fresh whole blood was obtained by venipuncture from volunteers who had no apparent inflammatory conditions and had not taken any NSAIDs for at least 2 weeks prior to blood collection. One millilitre aliquots were immediately transferred to eppendorff tubes containing 4 μL of vehicle (DMSO) or test compounds with concentrations ranging from 0.01 to 500 μM. The tubes were vortexed and incubated in 37 °C under constant agitation in a water bath for 1 h to induce spontaneous blood clot. At the end of the incubation the samples was centrifuged at 13,000 rpm for 5 min. Serum samples were collected and stored in eppendorf tubes at −20 °C. $TXB_2$ production was determined using an enzyme immuno-assay kit (Amershan Company) according to the manufacturer's instructions.

#### 4.4.2. In vitro COX-2 assay[22]

Fresh whole blood was obtained by venipuncture from volunteers in syringes containing heparin (10 UI/ml). One millilitre samples of blood were transferred to eppendorf tubes containing 4 μL of DMSO (vehicle) or test compounds to obtain concentrations ranging from 0.001 to 1000 μM. The tubes were vortexed and incubated under constant agitation in a water bath for 15 min followed by a new incubation with 20 μL of lipopolysaccharide (LPS) (Sigma–Aldrich, LPS from *Escherichia coli* serotype 055:B5) at a final concentration of 100 μg/ml under constant agitation during 5 h in order to stimulate COX-2 expression from blood monocytes. Appropriate controls were done replacing 20 μL of LPS by 20 μL of PBS. At the end of the incubation, the blood was centrifuged at 13,000 RPM for 5 min to obtain plasma. The plasma samples were collected and stored at −20 °C for further determination of $TXB_2$ using an enzyme immuno-assay kit (Amershan Company) according to the manufacturer's instructions.

#### 4.4.3. Formalin-induced pain in mice

The formalin induced pain test was carried out as described by Hunskaar and Hole.[36] Animals were injected subplantarly with 20 μL of 2.5% formalin in hind paw. LASSBio 930 (1c) and nimesulide were administered at a dose of 300 μmol/kg. The time that

mice spent licking or biting the injected paw or leg was recorded. Two distinct periods of intensive licking activity were identified and scored separately unless otherwise stated. The first period (earlier or neurogenic phase) was recorded 0–5 min after formalin injection and the second period (later or inflammatory phase) was recorded 15–30 min after injection.

### 4.5. Molecular modeling

#### 4.5.1. Selection of protein crystal structures

Ligand-bound crystal structures of COX-1 and COX-2 were retrieved from RCSB Protein Data Bank.[37] In this study, COX-1 crystal structure 1PXX and COX-2 crystal structure 1CX2 were evaluated and selected for docking.[24,25]

#### 4.5.2. Preparation of the ligands

The preparation of the ligands for docking with GOLD was performed using SYBYL version 8.0.[38] First, the ligand coordinates were generated using the program SKETCHER, available in SYBYL version 8.0. Next, the correct atom types (including hybridization states) and correct bond types were defined and hydrogen atoms were added. The energies of ligand structures were further minimized using the semiempirical AM1 method in SYBYL 8.0. PM3, AM1, MMFF94 and Gasteiger-Hückel charges were assigned to the ligand database.[38]

#### 4.5.3. Preparation of protein structures

Proteins were prepared for the docking studies using the Biopolymer module of SYBYL 8.0. AMBER7 FF99 charges were attributed to the protein atoms.[38] Biopolymer protein analysis tool was used, in a stepwise process of analysis and correction of geometry parameters. The assignment of hydrogen positions has been made on the basis of default rules. The side chains of lysine, arginine and the carboxylate groups of aspartic and glutamic acid have been modeled in their ionized states. Water molecules contained in the PDB file have been removed. Finally, the active site of the ensemble has been defined as the collection of residues within 20.0 Å of the hydroxyl oxygen atom of Tyr385.

#### 4.5.4. ChemScore fitness function

ChemScore is an empirical scoring function to estimate the free energy of ligand binding to protein. It uses simple contact terms to estimate lipophilic and metal–ligand binding contributions, including hydrogen bonding interactions. The detailed methodology by which ChemScore calculates the free energy of binding between protein and ligands has been described somewhere else.[27]

## Acknowledgements

The authors thank Central Analítica (IQ-UFRJ) for technical facilities and CAPES (BR), CNPq (BR), FAPERJ (BR), PRONEX (BR) and IMINOFAR (BR, #420.015/05-1) for financial support and fellowships.

## Supplementary data

Supplementary data associated with this article can be found, in the online version, at doi:10.1016/j.bmc.2008.12.045.

## References and notes

1. Nathan, C. *Nature* **2002**, *420*, 846.
2. Williams, M.; Kowaluk, E. A.; Arneric, S. P. *J. Med. Chem.* **1999**, *42*, 1481.
3. (a) Smith, W. L.; Meade, E. A.; DeWitt, D. L. *Ann. N.Y. Acad. Sci.* **1994**, *714*, 136; (b) Vane, J.; Bakhle, Y. S.; Botting, R. M. *Ann. Rev. Pharmacol. Toxicol.* **1998**, *38*, 97.
4. For a recent review, see: Fraga, C. A. M.; Barreiro, E. J. *Curr. Med. Chem.* **2006**, *13*, 167.
5. For recent examples, see: (a) Lima, P. C.; Lima, L. M.; da-Silva, K. C. M.; Léda, P. H. O.; Miranda, A. L. P.; Fraga, C. A. M.; Barreiro, E. J. *Eur. J. Med. Chem.* **2000**, *35*, 187; (b) Cunha, A. C.; Figueiredo, J. M.; Tributino, J. L. M.; Miranda, A. L. P.; Castro, H. C.; Zingali, R. B.; Fraga, C. A. M.; de-Souza, M. C. B. V.; Ferreira, V. F.; Barreiro, E. J. *Bioorg. Med. Chem.* **2003**, *11*, 2051; (c) Silva, G. A.; Costa, L. M. M.; Brito, F. C. F.; Miranda, A. L. P.; Barreiro, E. J.; Fraga, C. A. M. *Bioorg. Med. Chem.* **2004**, *12*, 3149; (d) Silva, A. G.; Zapata-Sudo, G.; Kummerle, A. E.; Fraga, C. A. M.; Barreiro, E. J.; Sudo, R. T. *Bioorg. Med. Chem.* **2005**, *13*, 3431; (e) Bezerra-Netto, H. J. C.; Lacerda, D. I.; Miranda, A. L. P.; Alves, H. M.; Barreiro, E. J.; Fraga, C. A. M. *Bioorg. Med. Chem.* **2006**, *14*, 7924; (f) Duarte, C. D.; Tributino, J. L. M.; Lacerda, D. I.; Martins, M. V.; Alexandre-Moreira, M. S.; Dutra, F.; Bechara, E. J. H.; De-Paula, F. S.; Goulart, M. O. F.; Ferreira, J.; Calixto, J. B.; Nunes, M. P.; Bertho, A. L.; Miranda, A. L. P.; Barreiro, E. J.; Fraga, C. A. M. *Bioorg. Med. Chem.* **2007**, *15*, 2421.
6. (a) Barreiro, E. J.; Fraga, C. A. M.; Miranda, A. L. P.; Rodrigues, C. R. *Quím. Nova* **2002**, *25*, 129; (b) Mahy, J. P.; Gaspard, S.; Mansuy, D. *Biochemistry* **1993**, *32*, 4014.
7. Lages, A. S.; Silva, K. C. M.; Miranda, A. L. P.; Fraga, C. A. M.; Barreiro, E. J. *Bioorg. Med. Chem. Lett.* **1998**, *8*, 183.
8. (a) Khanapure, S. P.; Garvey, D. S.; Young, D. V.; Ezawa, M.; Earl, R. A.; Gaston, R. D.; Fang, X.; Murty, M.; Martino, A.; Shumway, M.; Trocha, M.; Marek, P.; Tam, S. W.; Janero, D. R.; Letts, L. G. *J. Med. Chem.* **2003**, *46*, 5484; (b) Khanapure, S. P.; Augustyniak, M. E.; Earl, R. A.; Garvey, D. S.; Letts, L. G.; Martino, A. M.; Murty, M. G.; Schwalb, D. J.; Shumway, M. J.; Trocha, A. M.; Young, D. V.; Zemtseva, I. S.; Janero, D. R. *J. Med. Chem.* **2005**, *48*, 3930.
9. Duarte, C. D.; Barreiro, E. J.; Fraga, C. A. M. *Mini-Rev. Med. Chem.* **2007**, *7*, 1108.
10. Miranda, A. L. P; Lima, P. C.; Tributino, J. L. M.; Melo, P. A.; Fernandes, P. D.; Cintra, W. M.; Fraga, C. A. M.; Barreiro, E. J. *Abstracts of Papers*, 6ème Congrès Annuel de la Société Française de Pharmacologie, Rennes, France, 2002; P296.
11. Lima, L. M.; Barreiro, E. J. *Curr. Med. Chem.* **2005**, *12*, 23.
12. Barreiro, E. J.; Fraga, C. A. M. *Quím. Nova* **1999**, *22*, 744.
13. (a) Barreiro, E. J.; Lima, M. E. F. *J. Pharm. Sci.* **1992**, *81*, 1219; (b) Barreiro, E. J.; Costa, P. R. R.; Coelho, F. A. S.; De-Farias, F. M. C. *J. Chem. Res. (S)* **1985**, 220.
14. Ekeley, J. B.; Klemme, M. *J. Am. Chem. Soc.* **1928**, *50*, 2711.
15. Yamada, S.; Morizono, D.; Yamamoto, K. *Tetrahedron Lett.* **1992**, *33*, 4329.
16. Farrugia, L. J. *J. Appl. Crystallogr.* **1997**, *30*, 565.
17. Ferreira, S. H. *J. Pharm. Pharmacol.* **1979**, *31*, 648.
18. Rabasseda, X. *Drugs Today* **1996**, *32*, 365.
19. Seibert, K.; Zhang, Y.; Leahy, K.; Hauser, S.; Masferrer, J. L.; Perkins, W.; Lee, L.; Isakson, P. C. *Proc. Natl. Acad. Sci. U.S.A.* **1994**, *91*, 12013.
20. Smith, C. J.; Zhang, Y.; Koboldt, C. M.; Muhammad, J.; Zweifel, B. S.; Shaffer, A.; Talley, J. J.; Masferrer, J. L.; Seibert, K.; Isakson, P. C. *Proc. Natl. Acad. Sci. U.S.A.* **1998**, *95*, 13313.
21. Patrignani, P.; Panara, M. R.; Greco, A.; Fusco, O.; Natoli, C.; Iacobelli, S.; Cipollone, F.; Ganci, A.; Creminon, C.; MacLouf, J.; Patrono, C. *J. Pharmacol. Exp. Ther.* **1994**, *271*, 1705.
22. Young, J. M.; Panah, S.; Satchawatcharaphong, C.; Cheung, P. S. *Inflamm. Res.* **1996**, *45*, 246.
23. Rodrigues, C. R.; Veloso, M. P.; Verli, H.; Fraga, C. A. M.; Miranda, A. L. P.; Barreiro, E. J. *Curr. Med. Chem.* **2002**, *9*, 849.
24. Kiefer, J. R.; Pawlitz, J. L.; Moreland, K. T.; Stegeman, R. A.; Hood, W. F.; Gierse, J. K.; Stevens, A. M.; Goodwin, D. C.; Rowlinson, S. W.; Marnett, L. J.; Stallings, W. C.; Kurumbail, R. G. *Nature* **2000**, *405*, 97.
25. Kurumbail, R. G.; Stevens, A. M.; Gierse, J. K.; McDonald, J. J.; Stegeman, R. A.; Pak, J. Y.; Gildehaus, D.; Miyashiro, J. M.; Penning, T. D.; Seibert, K.; Isakson, P. C.; Stallings, W. C. *Nature* **1996**, *384*, 644.
26. Jones, G.; Willett, P.; Glen, R. C.; Leach, A. R.; Taylor, R. *J. Mol. Biol.* **1997**, *267*, 727.
27. Eldridge, M. D.; Murray, C. W.; Auton, T. R.; Paolini, G. V.; Mee, R. P. *J. Comp.-Aided Mol. Des.* **1997**, *11*, 425.
28. Enraf-Nonius COLLECT. Nonius BV, Delft, The Netherlands, 1997–2000.
29. Otwinowski, Z.; Minor, W.. In *Methods in Enzymology*; Carter, C. W., Jr., Sweet, R. M., Eds.; Academic Press: New York, 1997; Vol. 276, pp 307–326.
30. Sheldrick, G. M., SHELXS-97 *Program for Crystal Structure Resolution*; University of Göttingen: Germany, 1997.
31. Sheldrick, G. M., SHELXL-97 *Program for Crystal Structure Refinement*; University of Göttingen: Germany, 1997.
32. Farrugia, L. J. *J. Appl. Crystallogr.* **1999**, *32*, 837.
33. Bruno, I. J.; Cole, J. C.; Edgington, P. R.; Kessler, M. K.; Macrae, C. F.; McCabe, P.; Pearson, J.; Taylor, R. *Acta Crystallogr. Sect. B: Struct. Sci.* **2002**, *58*, 389.
34. Ribeiro, I. G.; Silva, K. C. M.; Parrini, S. C.; Miranda, A. L. P.; Fraga, C. A. M.; Barreiro, E. J. *Eur. J. Med. Chem.* **1998**, *33*, 225.
35. Lavich, T. R.; Cordeiro, R. S. B.; Silva, P. M. R.; Martins, M. A. *Braz. J. Med. Biol. Res.* **2005**, *38*, 445.
36. Hunskaar, S.; Berge, O.; Hole, K. *Pain* **1987**, *30*, 103.
37. Berman, H. M.; Westbrook, J.; Feng, Z.; Gilliland, G.; Bhat, T. N.; Weissig, H.; Shindyalov, I. N.; Bourne, P. E. *Nucleic Acids Res.* **2000**, *28*, 235.
38. SYBYL 8.0 ed., Tripos Inc., 1699 South Hanley Rd., St. Louis, Missouri, 63144, USA; http://www.tripos.com.